Evolutionary fuzzy logic system for intelligent fibre optic components assembly

D T Pham and M Castellani

Proceedings of the Institution of Mechanical Engineers, Part C: Journal of Mechanical Engineering Science 2002 216: 571
DOI: 10.1243/0954406021525359

Evolutionary fuzzy logic system for intelligent fibre optic components assembly

D T Pham* and **M Castellani**
Manufacturing Engineering Centre, School of Engineering, University of Wales, Cardiff, Wales, UK

Abstract: This paper presents a new evolutionary fuzzy logic system for use in the assembly of optical fibre components. The system optimizes the light output from a fibre by applying a gradient-based algorithm enhanced with momentum information. The parameters of the algorithm are adjusted on-line by a fuzzy controller according to the progress of the alignment process. The control knowledge base is automatically generated via a new evolutionary algorithm. The algorithm divides the population into three subgroups, each concerned with a different level of knowledge-base optimization, and employs a new adaptive selection routine that aims to keep the selection pressure constant throughout the learning phase. The resulting fuzzy logic controller demonstrated a robust performance with alignment times and accuracies comparing favourably against those obtained using a manually designed controller. Moreover, the evolved knowledge base was expressed in a transparent format that facilitated the understanding of the control policy.

Keywords: evolutionary algorithms, fuzzy logic, fibre optics, automatic assembly

NOTATION

$\boldsymbol{a}$	acceleration vector
$f(i)$	fitness value of individual i
$f'(i)$	normalized fitness value of individual i
fastest	individual fastest at locating the energy peak in a generation
$\boldsymbol{F}$	force vector
I_{ij}	membership function of fuzzy term j of input universe of discourse i
O_{ij}	membership function of fuzzy term j of output universe of discourse i
$m(i)$	mating chance of individual i
$\boldsymbol{r}$	position vector
steps	peak search steps
t	time
$\boldsymbol{v}$	velocity vector
ε	energy
μ	mass of body
κ	friction coefficient
τ	time

Abbreviations

EA	evolutionary algorithm
FL	fuzzy logic
KB	knowledge base
MF	membership function
RB	rule base

1 BACKGROUND

Fibre optic transmission is widely employed in modern high-bandwidth telecommunication systems. One of the greatest challenges in manufacturing fibre optic transmitters is to couple the light efficiently from the laser chip into the 9 μm diameter core of the fibre.

To match the laser spot size to the fibre core effectively, some kind of lens system is required [**1**, **2**]. All experiments in this study were carried out using the discrete lens alignment approach (see Fig. 1), where a focusing lens is embedded in the emitter frame to couple the light into the optical fibre. To achieve optimum light coupling the fibre must be positioned at a distance of a few mm from the laser chip, while the components have to be aligned with a precision better than 1 μm.

Current manufacturing technology does not allow the required submicrometre fibre alignment to be achieved by precision fitting of pre-formed components. It is therefore necessary to use an active alignment technique,

The MS was received on 12 April 2001 and was accepted after revision for publication on 16 January 2002.
** Corresponding author: Manufacturing Engineering Centre, School of Engineering, University of Wales, Cardiff, PO Box 925, Newport Road, Cardiff CF24 0YF, Wales, UK.*

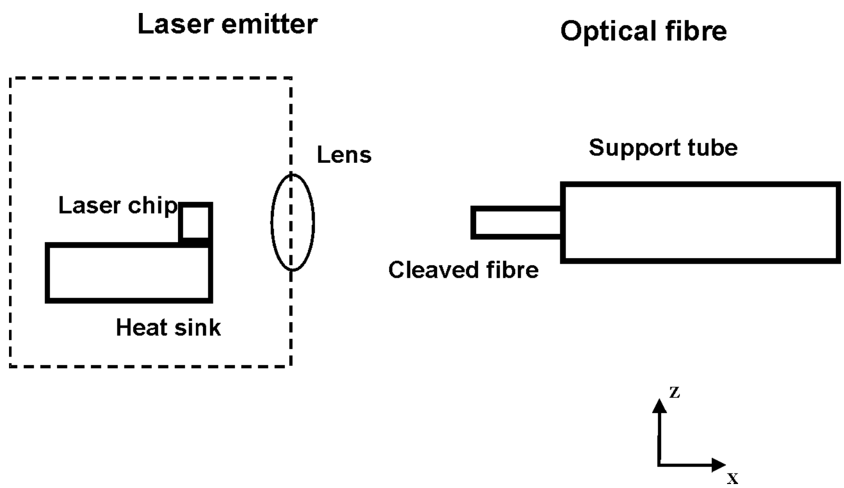

Fig. 1 Discrete lens configuration

where optimum light coupling is achieved by activating the laser chip and moving it relative to the fibre while monitoring the light output from the latter. When the maximum amount of light is obtained, the fibre assembly is permanently fixed relative to the laser chip using fast-setting adhesives or by laser welding.

At present, active alignment can be achieved either by using manual techniques or by automatic systems. In the first case, an operator controls a three-axis micrometre stage trying to maximize the fibre light output monitored on an optical powermeter display. This is a slow process, with a cycle time ranging from 2 to 5 min depending on the product being manufactured. Automatic techniques employ high-precision stepping motors to drive a three-axis stage on which the fibre assembly is mounted. A computer drives the motors and simultaneously measures the output of a powermeter attached to the fibre. A combination of area scans and gradient-based search routines is used for the localization of the energy peak.

The task is particularly complex as the laser beam seldom exhibits the ideal well-behaved single Gaussian energy spread. Rather, its energy distribution normally presents a main peak surrounded by a number of secondary peaks and other irregularities. The shape, location and peak value of the energy distribution depend on the laser emitter considered. The alignment is also complicated by positional inaccuracies of the stepping motors and mechanical vibrations of the frame.

Simple gradient-based algorithms can converge to suboptimal peaks and lengthy area scans and other techniques are necessary to ensure that the global energy maximum is found. The simple gradient approach results in the system making a large number of ‘move, stop and measure' cycles before the optimum position is reached. Recently, Pham and Castellani [**3**] introduced an improved peak search algorithm where the parameters of the gradient-based search were adjusted on-line via a fuzzy logic (FL) [**4**] control module. The new automatic system allowed a considerable reduction in the laser-to-fibre alignment times.

Although the construction of the knowledge base (KB) for the FL control module is conceptually straightforward, much effort is required manually to tune the fuzzy rules and membership functions (MFs) that make up the controller. This paper presents the application of an evolutionary algorithm (EA) developed by the authors [**5**] to the automatic generation of the KB for the laser-to-fibre alignment controller. Following an overview of the algorithm, its implementation in this problem is detailed together with the experimental results obtained.

2 OVERVIEW OF THE EVOLUTIONARY ALGORITHM

The evolutionary algorithm used in this work is described in reference [**5**]. For ease of referencing, this section gives a summary of the key features of the algorithm.

In its present configuration, the proposed EA is designed for the generation of Mamdani-type FL systems through simultaneous evolution of both the rule base (RB) and MFs. The shape of the fuzzy MFs has been fixed to be a trapezoid and is not subjected to learning. To increase KB transparency, no rule confidence factors are used in the fuzzy inferencing. For the sake of generality, their representation was included in the genome of the rules. Their value is set to one (i.e. full confidence, no action scaling) and is left unchanged by the evolutionary procedure.

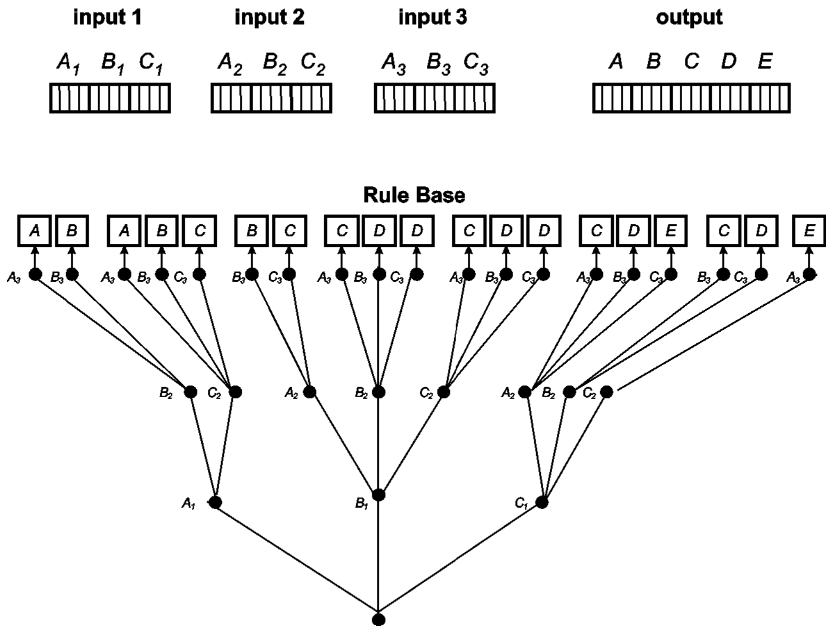

Fig. 2 Representation scheme

The algorithm uses the generational replacement reproduction scheme [**6**], a new selection operator [**5**] and a set of crossover and mutation procedures [**7**] dealing with different elements of the fuzzy KB to evolve a population of FL systems. The population is divided into three subgroups to which different operators are applied. A specific integer-valued gene marks the species of each individual.

The genetic operators acting on the first subpopulation work at the level of input and output fuzzy partitions. Crossover generates two new individuals by mixing the MFs of the two parents for each variable. Each parent transmits its RB to one of the offspring. Random chromosomic mutations can create new fuzzy terms, delete existing ones, or change the parameters defining the location and shape of an MF. Whenever genetic manipulations modify the set of MFs over which an RB is defined, a 'repair' algorithm translates the old rule conditions and actions into the new fuzzy terms. The subpopulation of fuzzy systems undergoing this set of operations is called *species_1*.

The operators manipulating the second subpopulation search for the optimal RB. Genetic crossover creates two individuals by exchanging sets of rules between the two parents. Each of the offspring inherits the input and the output space partitions from one of its parents. The mutation operator randomly changes the action of a fuzzy rule. To accommodate the new partitions, the conditions and actions of the swapped rules are translated into new linguistic terms. This group of solutions is named *species_2*.

The operators acting on the third subpopulation deal with all the components of the fuzzy KB. Genetic recombination swaps all the MFs and the rules contained in a randomly selected portion of the input and output spaces. Mutation can take any of the forms defined for the modification of *species_1* and *species_2* genotypes. This third group of individuals is referred to as *species_3*.

The above mutation operators function at the KB level. There is also a mutation operator at the species level that transforms one species into another.

The proposed algorithm represents candidate solutions using multichromosome variable-length genotypes. Figure 2 gives an example of an encoded solution for an FL system having three input variables, each partitioned into three linguistic terms, and one output variable partitioned into five fuzzy terms.

A separate chromosome is used to describe the partition of each input and output variable, each chromosome being composed of a number of genes equal to the number of linguistic terms. Each gene is a real-valued string encoding the parameters defining the location and the shape of one MF. Figure 3 details the MF encoding scheme.

The fuzzy RB is represented as a multilevel decision tree, the depth of the tree corresponding to the dimensionality of the input space. The rule antecedent is encoded in the full path leading to the consequent, each node being associated with a rule condition. The nodes at the last level of the decision tree represent the rule consequent and contain a fuzzy action for each output variable.

A flowchart of the complete algorithm is given in Fig. 4.

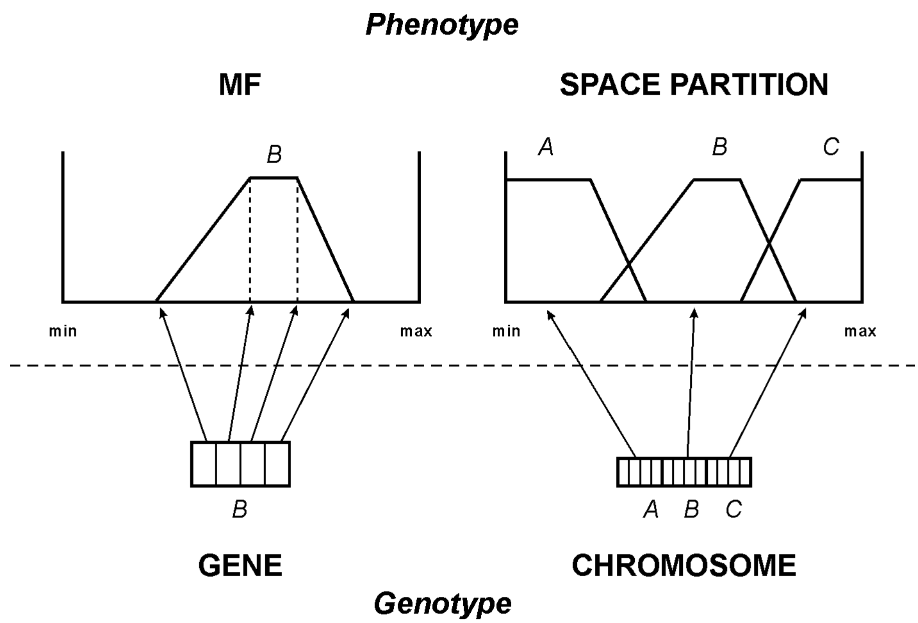

Fig. 3 MFs encoding

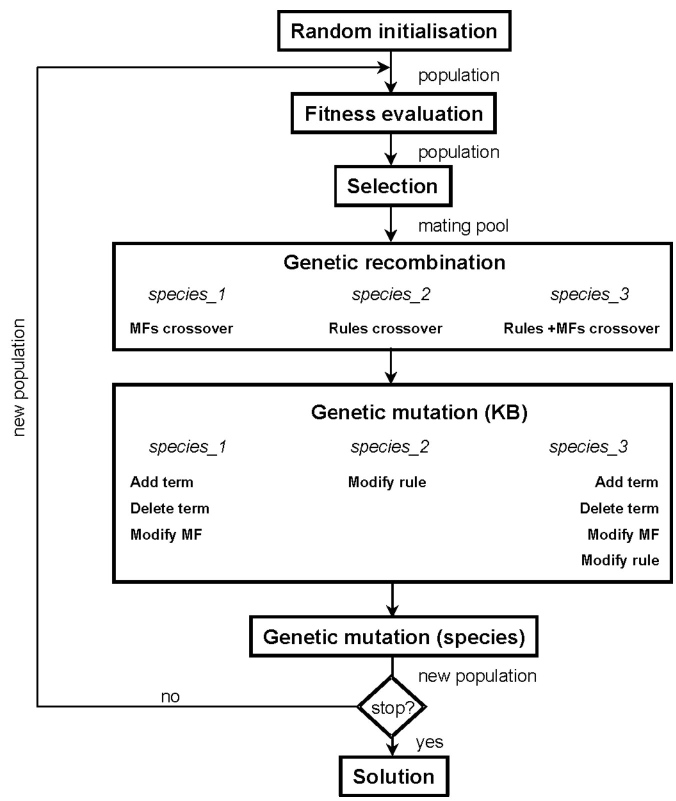

Fig. 4 Flowchart of proposed EA

3 CONTROL OF FIBRE OPTIC COMPONENTS ASSEMBLY

3.1 Problem domain

Aligning an optical fibre with a laser emitter to achieve optimum light coupling is essentially a search problem. The aim of the process is to locate the position where the laser beam intensity is maximum. Henceforth, a three-dimensional Cartesian reference frame XYZ will be assumed with X perpendicular to the surface of the transmitter and corresponding to the axis of the focusing lens. Z is taken to be vertical and pointing upwards (see Fig. 1). Figure 5 illustrates the evolution of

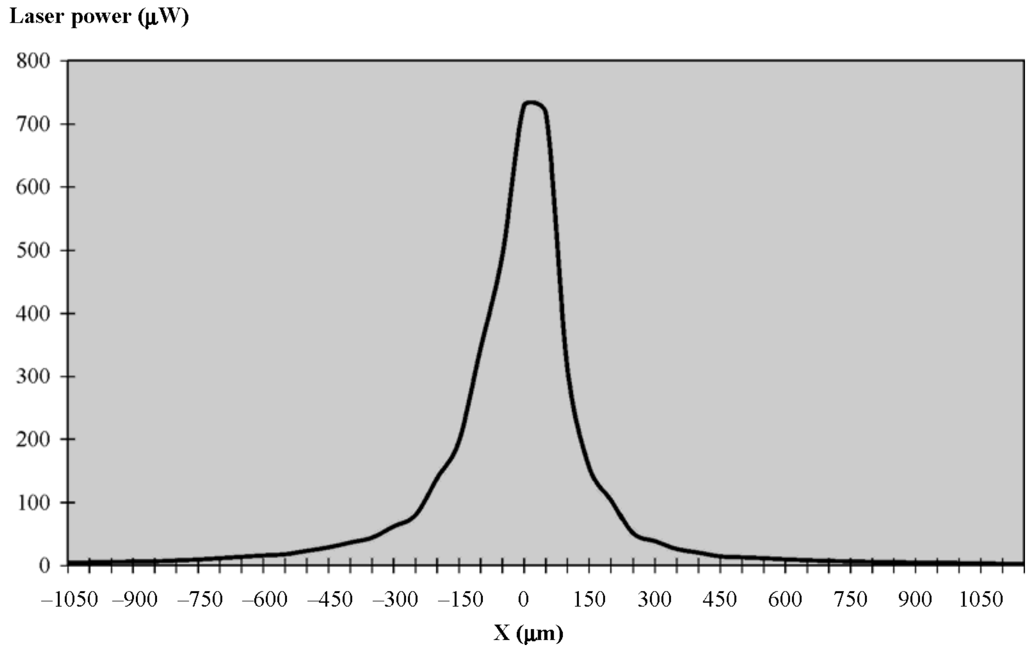

Fig. 5 Peak energy distribution along the focal axis

the peak energy value along the *X* reference axis for a sample laser emitter. Figure 6 shows the energy plot for a different laser emitter on the focal plane. Figures 7 and 8 respectively depict a secondary peak and a plateau in energy distributions sampled for different emitters on planes perpendicular to the focal axis.

The laser-to-fibre alignment algorithm developed by the authors [**3**] uses an enhanced gradient-based technique modelled upon the dynamics of a body travelling through a physical medium and experiencing the attractive force of a potential field. For convenience, the sign of energy readings from the optical powermeter is reversed, thus turning the problem into a surface minimization task.

The optical fibre is moved relative to the laser emitter according to the equations of motion of the body. The examples of a sphere falling down a valley and a meteorite attracted by the sun can help to visualize this strategy. Irregularities in real laser energy distributions can be pictured for the first example as flat areas, 'bumps' or 'potholes' along the hillside and in the second example as perturbations due to the gravita-

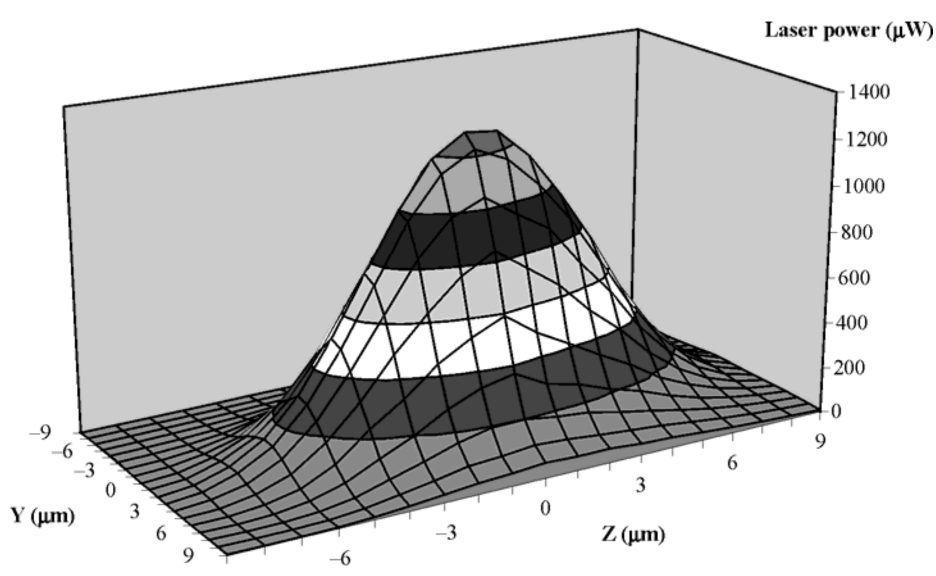

Fig. 6 Fine energy scan on the focal plane

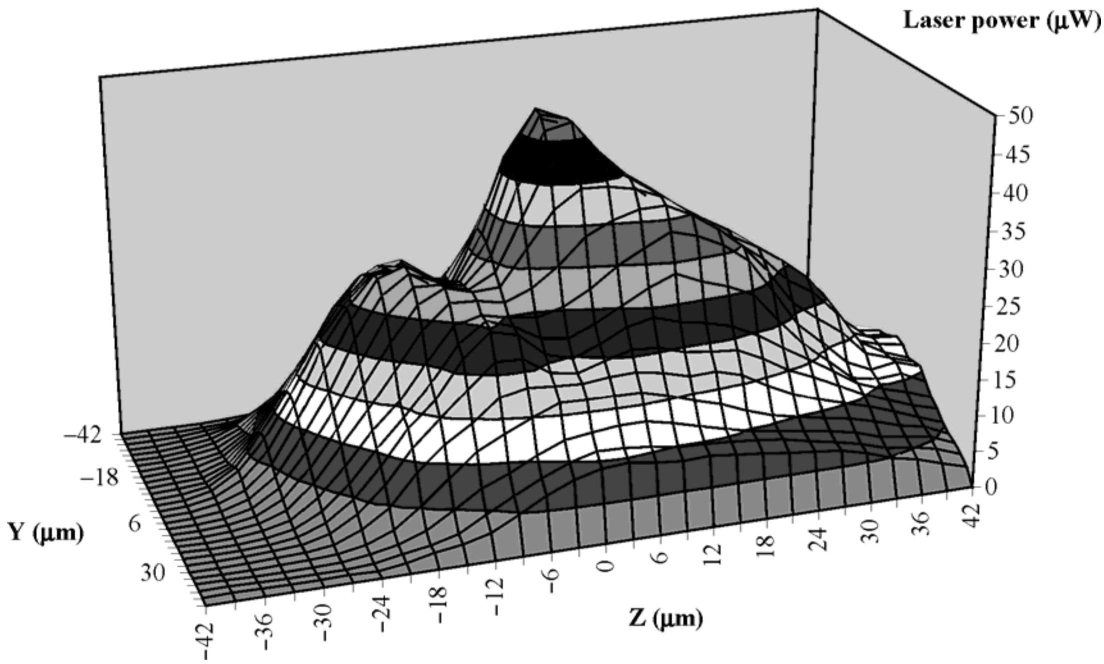

Fig. 7 A secondary peak at 800 μm from the focal point

tional fields of the various planets. The descent of the imaginary body down the energy slope is slowed down by friction.

The equations giving the motion of a body of mass μ in an attractive potential field and travelling in a medium of friction coefficient κ can be readily derived from classical physics. For a more detailed analysis, the reader is referred to reference [**3**]. Approximating the motion linearly for small movements and considering unitary time steps lead to the following equations:

$$\boldsymbol{a} = \frac{\boldsymbol{F}}{\mu} = -\frac{\Delta\varepsilon_0/\Delta\boldsymbol{r}_0 + \kappa \cdot \boldsymbol{v}_0}{\mu} \tag{1}$$

$$\boldsymbol{v} = \int \boldsymbol{a} \cdot \mathrm{d}\tau + \boldsymbol{v}_0 \approx \boldsymbol{a} \cdot \Delta\tau + \boldsymbol{v}_0 = \boldsymbol{a} + \boldsymbol{v}_0 \tag{2}$$

$$\Delta\boldsymbol{r} = \int (\boldsymbol{a} \cdot \Delta\tau + \boldsymbol{v}_0) \cdot \mathrm{d}\tau + \boldsymbol{r}_0 \approx \frac{\boldsymbol{a}}{2} + \boldsymbol{v}_0 \tag{3}$$

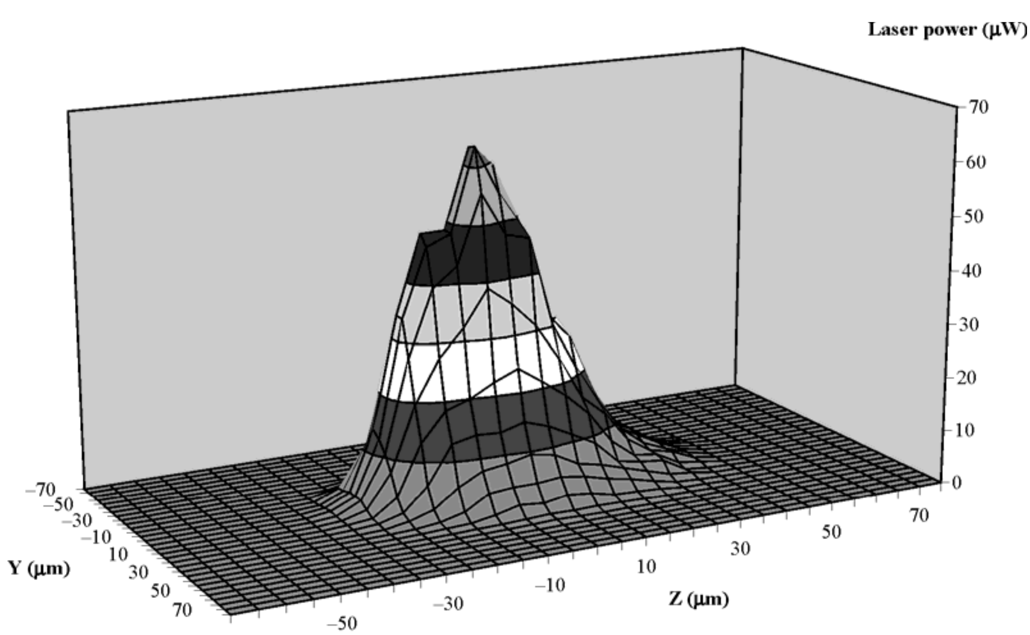

Fig. 8 A plateau at 400 μm from the focal point

where $\boldsymbol{a}$ is the body's acceleration, $\boldsymbol{v}$ is the body's velocity, $\boldsymbol{v}_0$ is the initial velocity, $\boldsymbol{r}$ is the body's position, $\boldsymbol{r}_0$ is the initial position, ε_0 is the potential energy of the field and $\mathrm{d}\tau \approx \Delta\tau = 1$ is the time interval.

Given μ and the ratio κ/μ, the displacement $\Delta\boldsymbol{r}$ of the body can be computed from the previous displacement $\Delta\boldsymbol{r}_0$ and the associated energy variation $\Delta\varepsilon_0$. Each $\Delta x, \Delta y$ and Δz motion component can be calculated by resolving the vectorial equations (1), (2) and (3) along the desired direction. For example, to obtain the Δx component, $\Delta\boldsymbol{r}$ and $\Delta\boldsymbol{r}_0$ must be replaced by Δx and $\Delta x_0, \boldsymbol{v}$ and $\boldsymbol{a}$ by v_x and a_x, and $\Delta\varepsilon_0$ with the energy change along the X direction. A system of nine equations will therefore completely determine the motion of the imaginary body.

Because the magnitude of the energy gradient along the focal axis was much smaller than along the other two directions, it was convenient to divide the search algorithm into two modules, one for the focal axis and the other for the Y and Z directions, to reduce the complexity of the controller. In the implementation of the fuzzy controller, the proposed gradient-based search algorithm was used only for optimizing the energy in the YZ planes. Once the maximum energy was found in a plane, the stage carrying the emitter was made to step a fixed distance along the X axis towards the fibre and the search was restarted in a new plane. The procedure was repeated until the YZ plane nearest to the focal point was found, i.e. the one where the peak value of the energy was highest. A final tuning of the position was performed, restarting the gradient-descent algorithm from the energy peak location. The X step size was set to 80 μm after an examination of the laser energy distribution from a batch of sample emitters. This measure allowed the focal plane to be determined with a precision of 40 μm, a value that did not substantially affect the peak energy value. As the energy gradient along the three coordinate directions is not known *a priori*, it is necessary to perform each motion component separately and measure the energy at the end of each step.

The search algorithm includes an initial scanning routine to locate a convenient starting point for the gradient descent. This point should be situated close enough to the main peak to minimize the alignment time and the risk of non-optimal convergence. On the other hand, the location of the starting point necessarily requires time consuming area scans. A trade-off is therefore necessary between search accuracy and scanning time.

The choice of the parameters μ and κ/μ is important for the effectiveness of the algorithm. Ideally, μ and κ/μ should be small in the presence of a small gradient in order to magnify the attraction force and let the body quickly descend the slope. On the other hand, as the energy decreases and the body approaches the energy minimum, larger values of μ and κ/μ are required to avoid excessive overshooting and oscillation around the minimum. For similar reasons, in the presence of a steep slope, a large mass and a high friction force will prevent excessive growth of the momentum term.

The proposed algorithm employs an FL system [**8, 9**] for the control of μ and κ/μ in each direction of motion. Besides the simplification of the control strategy, fuzzy logic is particularly suitable for the task because of its robustness to noise and the smoothness of its output characteristic [**10**]. The FL system has two inputs, the measure of the laser beam power and its change with time, and two outputs, μ and κ/μ. The EA outlined in the previous section is used automatically to generate the fuzzy KB for the control of μ and κ/μ.

3.2 EA settings

The settings of the EA parameters are summarized in Table 1. Parameters defined over a range of values were randomly initialized in the given interval. The sought solution had two inputs, the transmitted power ε and its time derivative, and two outputs, the control parameters μ and κ/μ. During the seeding of the initial population, for each variable, the universe of discourse was partitioned into five linguistic terms having equal support intervals and defining a normalized fuzzy partition. The extremes of the definition interval of the MFs of each variable were in some cases determined by problem-specific constraints (e.g. the maximum measurable power is 2000 μW or the minimum mass μ of the imaginary particle is 0 units) and in other cases randomly set constraints (e.g. the maximum μ value and the upper and lower extremes of $\Delta\varepsilon/\Delta t$).

If, during the evolutionary process, a solution experienced an input value outside the MF range, one of the two extreme terms had the support of its MF extended to include the new value. By initializing the terms of each solution around an interval of known feasible values, it was possible to evolve minimal fuzzy space partitions. This helped to reduce the search effort as well as minimizing the number of sets and rules. Also, to keep the solutions simple, a maximum of ten linguistic terms per universe of discourse was set. If in a genotype this number was exceeded, terms (i.e. genes) were randomly removed from the chromosome concerned until their number was regularized.

To prevent the generation of infeasible fuzzy rules, the starting population was initialized with a blank RB. During the fitness evaluation phase, all candidate solutions were tested for a certain number of time steps. At each step, a solution determined the set of fuzzy actions by searching its fuzzy decision tree for paths whose nodes were contained in the set of input conditions. In general, not all combinations of fuzzy conditions would lead to an existing rule action. At each time step, the proposed algorithm created a new path in

Table 1 Evolutionary FL controller—EA settings

EA parameters		
Population size	*pop*	60
Number of generations	*gen*	500
Number of runs	*iter*	3
Mutation rate (KB)	*mut_rate*	0.15
Mutation rate (species)	*mut_rate_species*	0.1
Maximum number of terms per variable	*max_terms*	10
Initialization settings		
Number of terms per variable	*init_terms*	5
Lower bound of space partition of ε	min_ε	50 μW
Upper bound of space partition of ε	max_ε	2000 μW
Range for lower bound of space partition of $d\varepsilon/dt$	$min\_d\varepsilon/dt$	(−450,−225) μW
Range for upper bound of space partition of $d\varepsilon/dt$	$max\_d\varepsilon/dt$	(225,450) μW
Lower bound of space partition of μ	min_μ	0
Range for upper bound of space partition of μ	max_μ	(3,6)
Lower bound of space partition of κ/μ	min_κ/μ	0
Upper bound of space partition of κ/μ	max_κ/μ	1
Rule base		Empty
Fitness function settings		
Maximum number of evaluation steps	τ	50
Minimum power value at peak	ε_{max}	500 μW
Minimum power reading at start of search	*threshold*	50 μW
Maximum X distance from peak at start of search	*max_X*	350 μm
Maximum Y/Z distance from peak at start of search	*max_YZ*	8 μm

the fuzzy decision tree if the set of input conditions having the highest matching degree did not result in a valid action. The rule consequent was randomly determined. The aim of the procedure was to limit the RB growth only to the most relevant instances. This feature allowed the creation of a minimal set of fuzzy rules but also emphasized the importance of the training procedure.

Once an individual was selected for mutation, the type of KB modification operator had to be chosen. For this purpose, a random procedure was used for *species_1* and *species_3* individuals, while solutions belonging to *species_2* could only undergo rule action modification. In the case of *species_1* individuals, the random procedure gave a 20 per cent probability for the addition of one fuzzy term, a 25 per cent chance for the deletion of one fuzzy term and the remaining 55 per cent probability for the modification of one fuzzy MF. The same operators were assigned half of these probability values when applied to *species_3* individuals, whereas the modification of a rule action had a 50 per cent chance. The allocation of these probabilities was according to practical experience, which also indicated that the best rate for the species mutation operator was 0.1.

The evolutionary procedure was run three times and each time the best solution was saved. At the end, the three saved solutions underwent a further evaluation stage to select the final solution. This repetition of the evolution process was introduced to reduce further the risk of a suboptimal result.

3.3 Fitness evaluation procedure

During the evolutionary search, the fitness of individual FL controllers was evaluated according to their precision and speed of locating the energy peak. It was not feasible to test the solutions on the real plant because of the long laser-to-fibre alignment times. Consequently, it was decided to employ a simulated alignment task based on an empirical model of the laser beam. The model was built by fitting three-dimensional energy scans of a batch of laser emitters. Because the characteristics of the beam varied widely with the source, the modelling effort was focused on the main features of the emission rather than the precise fitting of the acquired data. For the same reason, the sample of fibre optic components was not selected to be representative of the entire population.

For each individual, the search algorithm was run until either the peak was localized or a predefined number of steps τ had elapsed. The search starting point and the value of the energy peak were randomly varied every generation. The former was set to values guaranteed to be obtained during the preliminary energy scan. Once the algorithm had stopped, the final energy reading and the number of search steps were recorded. The fitness was then calculated as follows:

$$f(i) = \varepsilon_f + \frac{steps\ (fastest)}{steps(i)} \frac{\varepsilon_f}{10} \tag{4}$$

where $f(i)$ is the fitness of individual i, ε_f is the final energy reading, $steps(i)$ is the number of steps it took

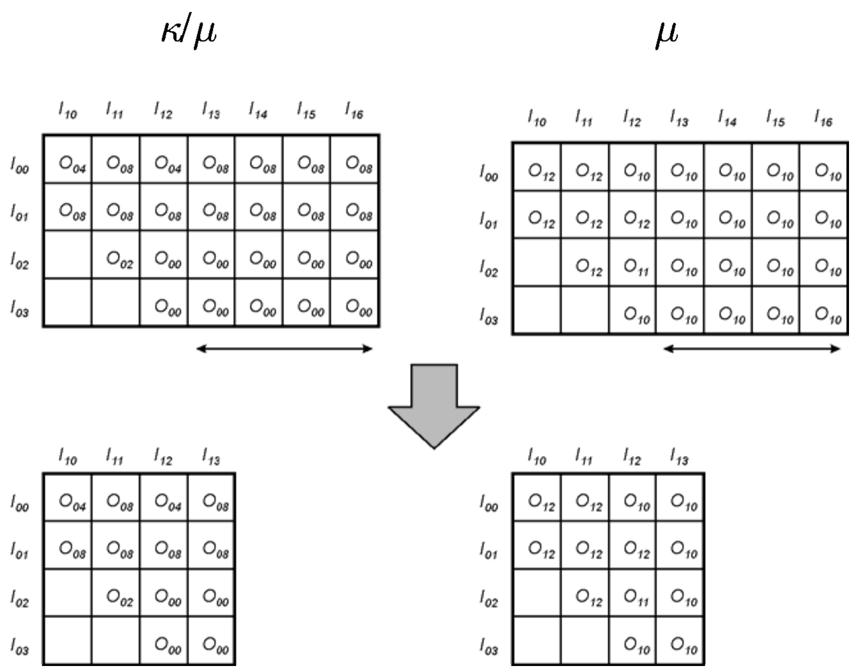

Fig. 9 RB simplification

individual i to locate the peak and *fastest* is the solution that localized the peak most quickly during that evaluation trial.

Equation (4) is composed of two terms related to the precision and the speed of the candidate solution. The contribution of the speed evaluation term has a magnitude 10 times smaller than the term expressing the precision. This was to bias the search first towards solutions able to locate the energy peak and then solutions allowing fast alignment.

4 ALIGNMENT RESULTS

Some first conclusions can be drawn by comparing the control KB produced by the proposed EA with the manually designed KB for the same control problem reported in reference [**3**]. In the automatically evolved KB, the input universes of energy and change in energy are respectively discretized into seven and four fuzzy terms, while the output universes of μ and κ/μ are respectively discretized into nine and three fuzzy terms. The fuzzy RB contains 25 production rules.

The manually created KB was slightly more compact in terms of fuzzy partitions and RB size. It divided the input space into 5×4 overlapping 'patches', each of them associated with a control response. The two output signals were created using five and four output terms respectively. On the other hand, the automatically evolved KB divided the input space into 7×4 overlapping patches, 25 of them associated with a control response. It therefore defined eight more input subareas and five more control rules. Also, the overall number of output fuzzy terms was greater, amounting to 9+3 terms.

Nevertheless, closer examination of the fuzzy response tables shows that, by applying some straightforward regrouping operations, the size of the learned fuzzy KB could be greatly reduced. The upper part of Fig. 9 depicts the fuzzy decision tables for the outputs of the two fuzzy systems. As indicated by the arrows, both tables have the same entries for the last four columns. It is therefore possible to merge terms I_{13} to I_{16} to obtain a 4×4 decision matrix (see the lower part of Fig. 9). Moreover, only four out of nine elements of the term set for the first output are actually used in the control rules. If needed, the introduction of manual or automatic pruning should therefore noticeably reduce the KB complexity. However, the complexity of the learned KB is acceptable, especially considering that the proposed EA does not contain any direct bias in favour of more compact solutions.

The EA-generated FL system was tested on the alignment of a batch of 40 different pairs of fibre optic components. For each alignment trial, a different laser emitter was used, while the optical fibre was changed every five trials. For each pair of components, the search algorithm was run until its completion or interrupted as soon as the power reading reached the maximum measurable value of 2000 μW. A combination of manual and conventional automated techniques were then used to search for further energy improvements. If the final energy peak value was not significantly different from

Table 2 Comparison of manually built and EA-generated controllers

	Using manually built FL controller (40 alignment trials)			Using EA-generated FL controller (40 alignment trials)		
	Initial scan	Peak search	Total	Initial scan	Peak search	Total
Average (s)	17.65	15.20	32.85	17.00	13.95	30.95
Worst (s)	40	27	60	40	24	60
σ (s)	8.36	5.91	10.93	8.75	5.88	11.29

the value obtained by the proposed automatic alignment system, the trial was considered to have succeeded.

The results obtained using the EA-generated fuzzy system were compared with those of an identical experiment carried out using the manually built FL controller described in reference [**3**]. The comparative data are presented in Table 2.

Both automatic alignment systems successfully located the energy peak in all the trials performed, suffering from slight occasional inaccuracies due to the imprecision of the stepping motors. The new fuzzy controller allowed better alignment times, giving an 8 per cent reduction on the original gradient-based search time. However, such an improvement should be moderated by the magnitude of the standard deviation of the measurements.

Figures 10 and 11 show two examples of alignment trials relating to different pairs of fibre optic components and performed using the EA-generated KB. The sharp energy steps mark the passage to a different YZ plane. The plots show that an average of 10–15 steps was needed for the power optimization on a YZ surface.

In the first case, the search had already started in the proximity of the focal plane. The algorithm unsuccessfully explored the two neighbouring surfaces for improvements and then returned to the initial YZ plane for the final adjustment of the position. In the second case, the algorithm started two planes away from the global optimum. The best surface was therefore the third plane scanned. This corresponded to the energy peak in the middle of the plot. A sharp energy drop marked the move to the next YZ plane, where the algorithm unsuccessfully looked for further improvements. A last small energy drop indicated the return to the previously explored plane for the final energy adjustment. The two examples of Figs 10 and 11 substantially replicate the observations made using the manually designed FL system [**3**].

The results of the experiments therefore gave further evidence of the effectiveness of the proposed laser-to-fibre alignment technique. They also proved the capability of the proposed EA to generate a sound KB for the control of the gradient-based optimization process. The results obtained using the automatically generated KB are comparable with those achievable by manual adjustment of the fuzzy control policy. However, the evolutionary technique requires much less problem domain knowledge. It is also easily reconfigurable to new types of components and it is fast. Throughout the experiments, the average EA running time on a desk-top personal computer operating at 300 MHz was less than 15 min. This figure compares favourably with the 8 h or more needed for the manual development of the control KB.

5 CONCLUSIONS AND FURTHER WORK

A new EA was used to generate the KB for a fuzzy controller in the assembly of fibre optic components. The proposed technique employs a new adaptive

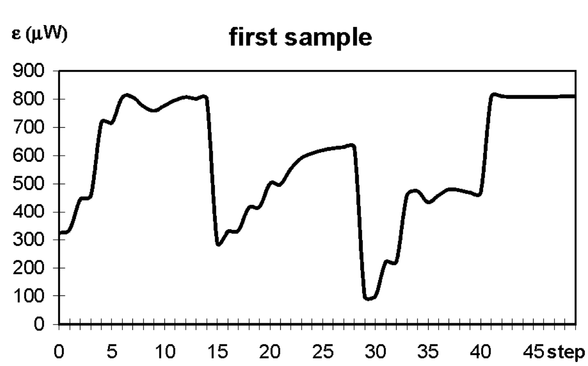

Fig. 10 EA-generated fuzzy system: power optimization curve 1

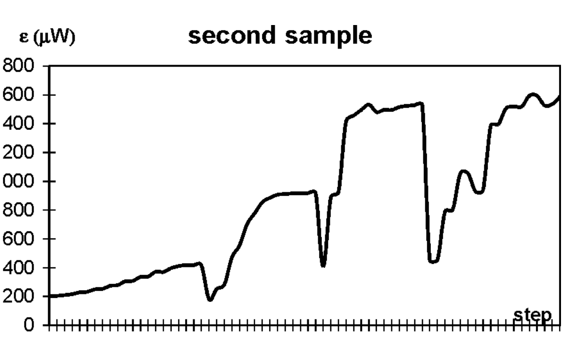

Fig. 11 EA-generated fuzzy system: power optimization curve 2

selection routine that aims to keep the selection pressure constant throughout the learning phase. The algorithm divides the population into three subgroups, each concerned with a different level of KB optimization. This allows the adaptive tuning of the disruptiveness and scope of the genetic manipulation operators.

The proposed learning technique generated an effective and reliable control policy. The evolved KB was expressed in a transparent format that facilitated the understanding of the policy. On the other hand, the proposed EA showed a tendency to produce redundant fuzzy terms and rules. Consequently, the generated KB was not as compact as a manually constructed KB although it was possible to reduce its size through tuning.

Further work should address the creation of automatic pruning routines capable of detecting and suppressing redundant KB elements. To minimize the computational burden, those routines could be invoked every fixed number of generations. Efforts spent on the inspection and adjustment of the solutions would be repaid by quicker processing of more compact solutions. It would also be worth while to investigate the possibility of adding an evolutionary bias towards simpler solutions. The main advantages of producing more compact solutions would be an increase in transparency of the control policy and simpler hardware and software implementation.

ACKNOWLEDGEMENTS

This research was sponsored by Agilent Technologies and the Welsh Assembly under the European Regional Development Fund programme. The authors would like to thank Mr M. S. Jones and Mr H. de Lacy of Agilent Technologies and Mr W. Jensen of Jensen Control and Robotics Engineering Limited for their expert technical support.

REFERENCES

1 **Geckeler, S.** *Optical Fiber Transmission Systems*, 1987 (Artech House, Norwood, Massachusetts).

2 **Gowar, J.** *Optical Communication Systems,* 2nd edition, 1993 (Prentice-Hall, New York).

3 **Pham, D. T.** and **Castellani, M.** Intelligent control of fibre optic components assembly. *Proc. Instn Mech. Engrs, Part B, Journal of Engineering Manufacture,* 2001, **215**(B9), 1177–1189.

4 **Zadeh, L. A.** Fuzzy sets. *Inf. and Control,* 1965, **8**, 338–353.

5 **Pham, D. T.** and **Castellani, M.** Outline of a new evolutionary algorithm for fuzzy systems learning. *Proc. Instn Mech. Engrs, Part C, Journal of Mechanical Engineering Science,* 2002, **216**(C5), 557–570.

6 **Davis, L.** *Handbook of Genetic Algorithms,* 1991 (Van Nostrand Reinhold, New York).

7 **Fogel, D. B.** *Evolutionary Computation: Toward a New Philosophy of Machine Intelligence,* 2nd edition, 2000 (IEEE Press, New York).

8 **Mamdani, E. H.** Application of fuzzy algorithms for control of simple dynamic plant. *Proc. IEE,* 1974, **121**(12), 1585–1588.

9 **von Altrock, C.** Successful fuzzy logic applications in industrial automation. In ISAEXPO '98, Proceedings of International Conference and Exposition on *Advances in Measurement and Control Technologies, Products and Services,* Houston, Texas, 1999, pp. 53–61.

10 **Lee, C. C.** Fuzzy logic in control systems: fuzzy logic controller, Parts I and II. *IEEE Trans. Systems, Man and Cybernetics,* 1990, **20**(2), 404–418 and 419–435.